Proceedings of 2004 IEEE/RSJ International Conference on
Intelligent Robots and Systems
September 28 - October 2, 2004, Sendai, Japan

Kalman Filtering for Real-Time Orientation Tracking of Handheld Microsurgical Instrument

Wei Tech Ang, Pradeep K. Khosla, and Cameron N. Riviere
The Robotics Institute
Carnegie Mellon University
Pittsburgh, USA

Abstract–**This paper presents the theory and modeling of a quaternion-based augmented state Kalman filter for real-time orientation tracking of a handheld microsurgical instrument equipped with a magnetometer-aided all-accelerometer inertial measurement unit (IMU). The on-board sensing system provides two complementary sources of orientation information. The all-accelerometer IMU provides a high resolution but drifting angular velocity estimate, while the magnetic North vector is combined with the estimated gravity vector to yield a non-drifting but noisy orientation estimate. Analysis of the dominant stochastic noise components of the sensors and derivation of the noise covariance are presented. The proposed Kalman filter obtains a non-drifting orientation estimate with improved resolution by incorporating the motion dynamics of the instrument during microsurgery and models the angular velocity drift explicitly as extra dynamic states.**

Keywords-Kalman filtering; quaternion; orientation tracking; inertial sensing; medical application

I. INTRODUCTION

Inertial sensing technology has been used extensively in aerospace navigation and in robotic motion sensing in the past few decades. In more recent years, there is an increasing interest in the application of inertial sensing technology to sense human movement, especially in the entertainment and medical applications.

To treat the notorious integrating drifts of inertial sensors, most of these applications employ a variation of Kalman filters and/or complimentary filters to perform real-time sensor fusion. These techniques typically use other on-board or external sensing sources to provide non-drifting references to bind the inertial sensor drifts.

Foxlin [1] presents two commercially available miniature inertial sensing systems for tracking head-mounted display in virtual reality applications. The core sensing module in both systems is made up of a triad of accelerometers, a triad of rate gyros, and a triad of magnetometers, called InertiaCube™. The InertiaCube™ is a three DOF orientation tracker that uses the gravity and the Earth's magnetic field as stationary references to correct for the drifts in the integrated tilt (roll and pitch) and pan (yaw) estimates from the gyros. Sensor fusion is performed via a separate bias complimentary Kalman filter [2]. The algorithm adopts a heuristic approach to ignore the accelerometers readings and rely solely on the gyros when the gravity estimation is corrupted by body movement. The process and measurement error covariance matrices and in turn the Kalman gains are computed, in the author's own words, in a 'sloppy' manner. The intrinsic sensor errors such as the bias and scale factor nonlinearity and temperature dependent variations are not explicitly modeled.

Bachmann *et al.* [3] and Yun *et al.* [4] invented the MARG (Magnetic (3 axes), Angular Rate (3 axes), and Gravity (3 axes)) sensors for tracking human body movements and apply these motion information to control human models in virtual environment. The sensor unit is completed with an on-board microcontroller and signal conditioning circuitry. Taking advantage of the numerical properties of quaternion orientation representation, a quaternion-based Kalman filter is implemented to fuse the information from the vector of nine sensors. To avoid the computational load of solving the nonlinear measurement equations, the authors adopted a numerical approach proposed by Gebre-Egziabher [5] to obtain the quaternions using Gauss-Newton method. Estimation of the gravity vector is by averaging the accelerometer outputs over an unspecified period of time, on the assumption that human movements do not produce constant linear acceleration. The gyro error dynamic is assumed to follow a Gauss-Markov model, but the computation and propagation of error covariance matrices has not been discussed and the Kalman gains are determined through experimental 'tweaking'. Bias and scale factor of each sensor are modeled using linear models.

Other Kalman filtering implementations in human motion tracking with a conventional three-gyro, three-accelerometer inertial measurement unit (IMU) include Rehbinder and Hu [6] and Luinge [7]. Without complementary sensors in the pan or yaw DOF, drift in the heading estimate will be inevitable.

In our ongoing effort in implementing active tremor compensation in a completely handheld microsurgical instrument [8], we have designed and implemented a six DOF all-accelerometer IMU [9] with superior angular sensing resolution. To bind the pan DOF sensor drift, a three-axis magnetometer has been subsequently added to the sensor suite. Deterministic errors of the accelerometers are modeled by a phenomenological method [10], and the proposed physical model reduces the time-independent error components, namely the nonlinearity and cross-axis effects, in the bias and scale factor to the level of stochastic white noise. The dominant noise components of the sensors are analyzed by the Allan variance method. This paper presents the theory and modeling of an augmented-state

0-7803-8463-6/04/$20.00 ©2004 IEEE

quaternion-based Kalman filter to perform real-time orientation tracking of the instrument.

II. Magnetometer-Aided All-Accelerometer Inertial Measurement Unit for Intelligent Handheld Microsurgical Instrument

A. Background

We have designed and implemented an intelligent handheld microsurgical instrument that senses its own motion, distinguishes between the intended and erroneous motion, and manipulates its tip in real-time to cancel the erroneous component. The current prototype is targeted at vitreoretinal microsurgery. The most familiar type of erroneous hand movement hampering healthy human micromanipulation performance is physiological tremor. Tremor is defined as a roughly sinusoidal motion, characterized by frequency typically in the band of 8-12 Hz. Physiological tremor in vitreoretinal microsurgery is found to have an amplitude of up to 50 μm rms in each principal direction [11].

B. Design

The sensing system of the active microsurgical instrument consists of three dual-axis miniature MEMS accelerometer (ADXL-203, Analog Devices Inc., MA, USA) and a three-axis magnetometer (HMC-2003, Honeywell Inc., NJ, USA) as shown in Figure 1.

It has been shown in [9] that this all-accelerometer IMU design yields superior angular sensing resolutions that are two orders of magnitude better than miniature low cost rate gyros (Tokin CG-16D, Japan) in the *X*- and *Y*-sensing DOF, and an order of magnitude better in the *Z*-sensing DOF.

While the all-accelerometer IMU makes possible the sensing of very small and slow angular motion that would otherwise be buried under the noise floor of low cost miniature gyros, it suffers from a faster orientation error growth rate than a conventional IMU with three gyros. This is because the angular motion estimate from the all-accelerometer IMU involves both the angular velocity and angular acceleration vectors. The inclusion of angular acceleration term introduces integrated noise or drift over time. The differential sensing kinematics algorithm to extract the body angular velocity vector will be discussed in the next section.

The addition of the three-axis magnetometer to the sensor suite allows us to form two complementary orientation sensing sources. On one hand, we have the all-accelerometer IMU with very high sensing resolution but poor long term sensing accuracy. On the other hand, the magnetic North vector may be combined with the gravity vector to provide non-drifting but low resolution orientation estimates. The poor sensing resolution is a result of the noisy magnetometer and the residual body acceleration of the instrument in estimating the gravity vector. Sensor fusion of these two sensing sources to obtain a high resolution, non-drifting orientation estimate forms the subject matter of the paper.

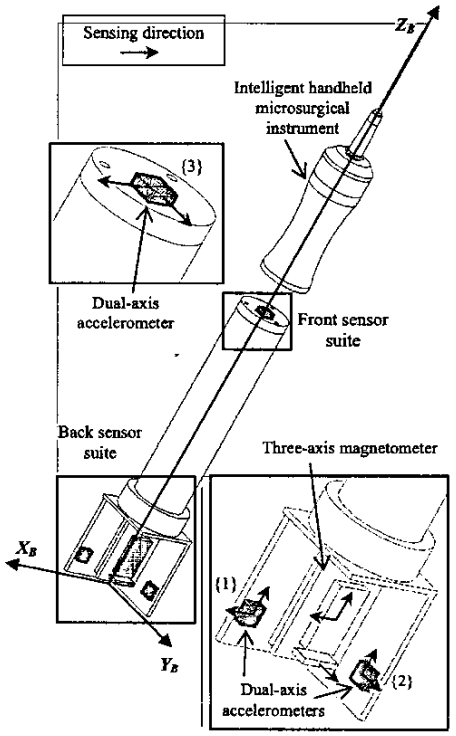

Figure 1 Design of the magnetometer-aided all-accelerometer inertial measurement unit in a handheld microsurgical instrument. The sensors are housed in two locations. The back sensor suite houses a three-axis magnetometer and two dual-axis accelerometers ({1}: 1 *X*- and 1*Z*-sensing; {2}: 1 *Y*- and 1 *Z*-sensing), and the front sensor suite houses a dual-axis accelerometer ({3}: 1 *X*-, 1 *Y*-sensing).

C. Differential Sensing Kinematics

To extract angular motion information from the all-accelerometer IMU, we took the difference between the sensed accelerations at different sensor locations. The difference in acceleration between locations $\{i\}$ and $\{j\}$ on a rigid body is due solely to two rotation-induced acceleration terms: centripetal and tangential accelerations,

$$
\begin{aligned}
{}^{B}A_{ij} &= {}^{B}A_j - {}^{B}A_i \\
&= \left({}^{B}\Omega_{\times}\cdot{}^{B}\Omega_{\times} + {}^{B}\dot{\Omega}_{\times}\right){}^{B}P_{ij}, \; i,j = 1,2,3,
\end{aligned} \tag{1}
$$

where ${}^{B}\Omega_{\times}$ and ${}^{B}\dot{\Omega}_{\times}$ are the skewed symmetric cross product matrix of the angular velocity vector ${}^{B}\Omega = [\omega_x \;\; \omega_y \;\; \omega_z]^T$ and the angular acceleration vector ${}^{B}\dot{\Omega}$ respectively,

$$
{}^{B}\Omega_{\times} = \begin{bmatrix} 0 & -\omega_z & \omega_y \\ \omega_z & 0 & -\omega_x \\ -\omega_y & \omega_x & 0 \end{bmatrix}, \; {}^{B}\dot{\Omega}_{\times} = \begin{bmatrix} 0 & -\dot{\omega}_z & \dot{\omega}_y \\ \dot{\omega}_z & 0 & -\dot{\omega}_x \\ -\dot{\omega}_y & \dot{\omega}_x & 0 \end{bmatrix}, \tag{2}
$$

and ${}^{B}P_{ij}$ is the position vector from $\{i\}$ to $\{j\}$, with respect to the body frame $\{B\}$. With well defined initial condition, ${}^{B}\dot{\Omega}$ may be expressed in terms of ${}^{B}\Omega$,

$$ {}^{B}\dot{\Omega}(t) = \frac{{}^{B}\Omega(t) - {}^{B}\Omega(t-T)}{T}, {}^{B}\Omega(0) = 0_{3\times 1}, \quad (3) $$

where T is the sampling period.

Since the accelerometer at each location senses two axes of motion, there are only three pairs of defined differential acceleration, one in each principal body axis,

$$ A_D = [a_{13x} \;\; a_{23y} \;\; a_{12z}]^T. \quad (4) $$

Hence, we have a system of three nonlinear equations with three unknowns,

$$ \begin{bmatrix} f_1 \\ f_2 \\ f_3 \end{bmatrix} = \begin{bmatrix} a_{13x} \\ a_{23y} \\ a_{12z} \end{bmatrix} - \begin{bmatrix} \left({}^{B}\Omega_x \cdot {}^{B}\Omega_x + {}^{B}\dot{\Omega}_x \right) {}^{B}P_{13}\big|_x \\ \left({}^{B}\Omega_x \cdot {}^{B}\Omega_x + {}^{B}\dot{\Omega}_x \right) {}^{B}P_{23}\big|_y \\ \left({}^{B}\Omega_x \cdot {}^{B}\Omega_x + {}^{B}\dot{\Omega}_x \right) {}^{B}P_{12}\big|_z \end{bmatrix}. \quad (5) $$

The angular velocity vector ${}^{B}\Omega$ may be found by solving (5) by nonlinear least-squares solver such as the Gauss-Newton or the Levenberg-Marquart method,

$$ \min\left\{ r({}^{B}\Omega) : {}^{B}\Omega \in \Re^3 \right\}, \; r({}^{B}\Omega) = \tfrac{1}{2} \left\| \bar{f}({}^{B}\Omega) \right\|_2^2, $$

$$ \bar{f}({}^{B}\Omega) = \begin{bmatrix} f_1 & f_2 & f_3 \end{bmatrix}^T. \quad (6) $$

D. TRIAD Algorithm

1) The Wahba's Problem. The determination of orientation of a rigid body from vector observations is also known as the Wahba's problem.

The original problem proposed by Wahba in 1965 was on the estimation of a satellite's attitude based on direction cosines of objects as observed in the satellite body frame and direction cosines of the same objects in a known frame of reference [12]. In other words, it is to find the orthonormal direction cosine or rotation matrix M that minimizes in the least squares sense the error function,

$$ \mathrm{E}(M) = \sum_{j=1}^{n} \left\| v_j^* - M v_j \right\|^2, \quad (7) $$

where $\{v_j^*\}$ is a set of unit vectors measured in the body frame and $\{v_j\}$ are the corresponding unit vectors in a reference frame. Examples of these vectors may be the unit vectors pointing to the direction of a specific star such as the Sun, the Earth's magnetic field or gravity, etc. The solution of the Wahba's problem yields non-drifting attitude estimate. Equation (7) is presented in Wahba's original notations.

Recasting the Wahba's problem in the context of orientation tracking with magnetometer-aided inertial measurement unit, the sensors measure in the body frame the gravity vector and the magnetic North vector, the solution to the problem gives the orientation of the body with respect to the world frame. Two non-collinear and non-zero length vectors is the minimum requirement to solve the Wahba's problem unambiguously.

Gebre-Egziabher [5] formulates an iterated least squares algorithm to solve for the error quaternion, and the error quaternion is cast into a standard linearized measurement equation of a complementary Kalman filter. In the recent development of the MARG sensor, Yun *et al.* [4] follow Gebre-Egziabher's approach to the Wahba's problem but compound the error quaternion with the gyros updated quaternion and express this quantity as the measurement states of a Kalman filter. The authors state computational efficiency as the primary reason of adopting this algorithm over their previous implementation [13].

2) The TRIAD Algorithm. Among the proposed solutions, the TRIAD algorithm [14] is the simplest and best suited for a two-vector Wahba's problem, despite its inefficiency in solving the general case with three or more observed vectors when compare to other methods [15]-[17].

We define the world coordinate system $\{W\}$ such that the z_W axis aligns with the negated gravity vector G, the x_W axis forms a plane with z_W that contains the magnetic North vector N, and the y_W axis completes the right-handed coordinate system. Hence, the gravity and the unit magnetic North vector in $\{W\}$ are defined as

$$ G = \|G\|[0 \;\; 0 \;\; -1]^T; \quad N = [n_x \;\; 0 \;\; n_z]^T. \quad (8) $$

The accelerometers and magnetometers sense the gravity and the unit magnetic North vector in the body frame $\{B\}$,

$$ {}^{B}G = [{}^{B}g_x \;\; {}^{B}g_y \;\; {}^{B}g_z]^T; \quad {}^{B}N = [{}^{B}n_x \;\; {}^{B}n_y \;\; {}^{B}n_z]^T. \quad (9) $$

The z_W axis in the body frame is simply

$$ {}^{B}z_W = -{}^{B}G / \|{}^{B}G\|. \quad (10) $$

Normalizing the cross product between ${}^{B}z_W$ and ${}^{B}N$ will give the y_W axis in the body frame,

$$ {}^{B}y_W = \frac{{}^{B}z_W \times {}^{B}N}{\left\| {}^{B}z_W \times {}^{B}N \right\|}. \quad (11) $$

A second cross product between ${}^{B}y_W$ and ${}^{B}z_W$ will yield x_W in the body frame,

$$ {}^{B}x_W = {}^{B}y_W \times {}^{B}z_W. \quad (12) $$

The direction cosines of the world frame $\{W\}$ with respect to the body frame $\{B\}$ is thus,

$$ {}^{W}C_B = \left[{}^{B}x_W \;\; {}^{B}y_W \;\; {}^{B}z_W \right]^T. \quad (13) $$

3) Gravity Vector Estimation. The TRIAD algorithm assumes a well-defined gravity vector, which is not readily available for a body in continuous motion. However, the body acceleration of the instrument during microsurgery is typically two orders of magnitude smaller than the gravity vector. Therefore, approximating the gravity vector with the raw accelerometer outputs would give a reasonably high quality estimate of about 1% error.

Acceleration content of the instrument in operation includes a high frequency (8-12 Hz) tremulous motion component and a low frequency (< 1 Hz) motion component, made up of primary the voluntary hand movement and other non-tremulous physiological errors. The corruption of the gravity estimate by these components results in a noise process characterized by superimposed white and colored noise sequences. A formal treatment of the colored noise is to model it as a bias and augment the Kalman filter with extra states. For ease of implementation, we assume the gravity noise vector to be white noise

processes. The consequence of this assumption is that the state estimates of the Kalman filter will become suboptimal.

III. Sensor Signal Processing

The proposed sensor signal processing for the magnetometer-aided all-accelerometer inertial measurement unit is depicted in Fig. 2. There are two categories of sensing errors for any sensing systems: deterministic error and stochastic error. The sensor outputs are first corrected for the deterministic errors, then the differential sensing kinematics and the TRIAD algorithms compute the body angular velocity vector and the direction cosine matrix, and finally they are fused by the augmented state quaternion-based Kalman filter based on their stochastic error characteristics.

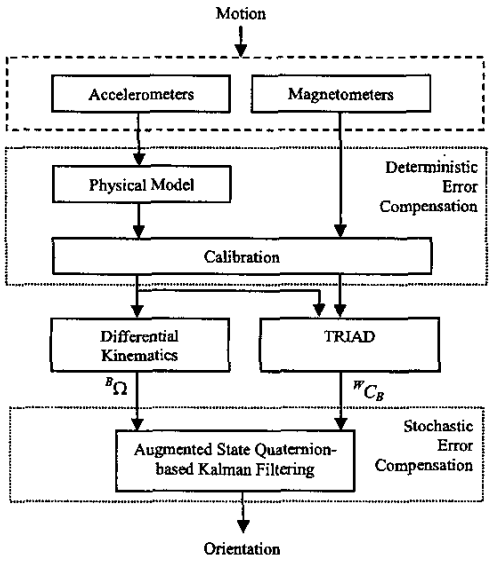

Figure 2 The proposed sensor signal processing for the magnetometer-aided all-accelerometer inertial measurement unit.

A. Deterministic Errors

We have proposed in our previous work [10] a physical model to explicitly model the deterministic errors inherent to the construction of the Analog Devices ADXL-203 dual-axis accelerometers. These errors include bias and scale factor errors due to nonlinearity, hysteresis, and cross-axis effects. It has been shown that the proposed physical model reduces the sensing error to the limit of random noise.

Scale factor of the magnetometer is irrelevant our application since the magnetometer measurement is normalized to obtain a directional unit vector and the absolute magnetic field strength is assumed to be constant through out the operation. The magnetometer bias is immune to motion, as long as the magnetic field and the relative position of ferrous material in close proximity remain unchanged.

Modeling of the orientation and position misalignment errors of the accelerometers and magnetometers should be examined at a system's level with respect to the body frame of the instrument. The calibration procedure is to be reported in a separate paper, and without loss of generality of the subject matter of this paper, we assume that the misalignment errors may be sufficiently compensated.

B. Stochastic Errors

Time varying and random errors are identified from the Allan variance analysis. Allan variance is a time domain system error analysis to identify dominant random drift components and their coefficients [18].

The accelerometers are left motionless and the outputs are recorded for 12 hours at 1 Hz. Allan variance analysis of the recordings reveals that the dominant stochastic noise components of the accelerometers are velocity random walk (white noise in acceleration) and acceleration random walk (white noise in jerk or integrated white noise); two of the three accelerometers (both axes) tested also exhibit bias instability or trend. Performing the analysis again on the final 4 hours of the same data set, trend disappears from the root Allan variance plots of these four axes. This finding is consistent with the experimental observation in [11], where the accelerometers experience bias and scale factor drifts over time and reach a steady state after a few hours. This is believed to be due to the gradual heating up of the sensor internal circuitry. Barshan *et al.* [19] proposes to use an exponential function to model the bias drift and implement the drift correction via an augmented state extended Kalman filtering. However, this approach is subjected to potentially large modeling error because the drift characteristics of the sensors are inconsistent and non-repeatable between operations. Moreover, quantifying this error may involve impractically great experimental effort.

In a subsequent experiment, outputs of the accelerometers after they reach steady state are recorded for 30 minutes, at 500 Hz. The data collection period of 30 minutes is the typical duration of a vitreoretinal microsurgery, our targeted application; and 500 Hz is the sampling rate of our system in operation. Allan variance analysis shows that the dominant stochastic noise components of the accelerometers are velocity random walk and acceleration random walk.

Experiments on the Honeywell HMC-2003 three-axis magnetometer show that it exhibits only a dominant white noise component.

IV. Augmented State Quaternion-Based Kalman Filtering

A. Orientation Representation

The lack of physical intuition in the quaternion orientation representation notwithstanding, it has been very well received in the aerospace navigation community because of its numerical advantages. The quaternion

eliminates the singularity problem and computational inefficiency associated with solving the transcendental equations in the Euler angles representation. Moreover, quaternion is robust against numerical errors that crept into the direction cosine matrix when updated by numerical integration methods, as a consequence of truncation, rounding off and commutation. It has been shown that quaternion-based direction cosine matrix has intrinsically zero skew error, negligible drift error with a second order integration method, and a scale error that is easily correctable by normalizing the quaternion [20].

The quaternion is defined as

$$Q = [q_0 \quad \bar{q}]^T, \tag{14}$$

where

$$q_0 = \cos\left(\tfrac{1}{2}\|\Theta\|\right),$$

$$\bar{q} = [q_1 \quad q_2 \quad q_3]^T = \sin\left(\tfrac{1}{2}\|\Theta\|\right)\frac{\Theta}{\|\Theta\|},$$

$$\Theta = \Omega T = [\theta_x \quad \theta_y \quad \theta_z]^T. \tag{15}$$

The unit vector $\Theta/\|\Theta\|$ is the axis of rotation and $\|\Theta\|$ is the angle of rotation, in the axis-angle representation. The quaternion has three DOF and satisfies the constraint

$$Q^T Q = 1. \tag{16}$$

B. Angular Velocity Bias Vector

We have discussed in the Section II-B that the body angular velocity vector ${}^B\Omega$ derived from the differential sensing kinematics algorithm is corrupted by an integrated drift. This drift may be treated as a bias. Thus, the true body angular velocity vector Ω is related to ${}^B\Omega$ by

$$\Omega = {}^B\Omega - B - \xi_\Omega, \tag{17}$$

where ξ_Ω is a vector of transformed zero mean Gaussian white noise processes that drives the angular velocity vector, and B is angular velocity bias vector assumed to be driven by transformed integrated Gaussian white noise processes,

$$\dot{B}(t) = \xi_B(t), \tag{18}$$

Although the noise vectors ξ_Ω and ξ_B are no longer Gaussian after nonlinear transformations, they are assumed to remain Gaussian for ease of implementation, the consequence is that the estimation will be suboptimal. Noise vectors ξ_Ω and ξ_B are assumed to be uncorrelated. The derivation of the covariance matrices of ξ_Ω and ξ_B will be discussed in Section IV-D.

C. The Process Model

1) State Vector. The state vector is selected to be the 4-tuple quaternion Q, augmented with the bias vector B of the body angular velocity,

$$x(t) = [Q(t)_{4\times1} \quad B(t)_{3\times1}]^T. \tag{19}$$

It can be shown that the quaternion is related to the angular velocity bias vector by the differential equation

$$\dot{Q}(t) = \tfrac{1}{2}\tilde{\Omega}_\times\left({}^B\Omega(t) - B(t) - \xi_\Omega(t)\right)Q(t), \tag{20}$$

where

$$\tilde{\Omega}_\times = \left[\begin{array}{c|c} 0 & -\Omega^T \\ \hline \Omega & \Omega_\times \end{array}\right], \tag{21}$$

and $\Omega_\times$ is the cross product matrix of Ω, which is defined in (17) and (18). Equation (20) may be rewritten as

$$\dot{Q}(t) = \tfrac{1}{2}\tilde{\Omega}_\times\left({}^B\Omega(t) - \xi_1(t)\right)Q(t) - \tfrac{1}{2}\tilde{Q}(t)B(t), \tag{22}$$

since $\tilde{\Omega}_\times$ is linear and homogeneous in its argument,

$$\tilde{\Omega}_\times(B)Q = \tilde{Q}B, \tag{23}$$

$$\tilde{Q} = \begin{bmatrix} q_0 & -q_3 & q_2 \\ q_3 & q_0 & -q_1 \\ -q_2 & q_1 & q_0 \\ -q_1 & -q_2 & -q_3 \end{bmatrix}. \tag{24}$$

Derivation and properties of (24) can be found in [21].

2) Discrete State Equation. Assuming the angular displacement is small and a constant angular acceleration motion model within one sampling period, the discrete state dynamic equation or process model is defined as

$$x[k] = \Phi[k]x[k-1] + \Psi[k]w[k] \tag{25}$$

where the state transition matrix is given by

$$\Phi = \left[\begin{array}{c|c} \Phi_{Q(4\times4)} & \Phi_{B(4\times3)} \\ \hline 0_{(3\times4)} & I_{(3\times3)} \end{array}\right]; \tag{26}$$

$$\Phi_Q = \cos\left(\tfrac{1}{2}\|\Theta\|\right)I_{(4\times4)} + \frac{\sin\left(\tfrac{1}{2}\|\Theta\|\right)}{\|\Theta\|}\tilde{\Theta}_\times,\ \tilde{\Theta}_\times = \tilde{\Omega}_\times T; \tag{27}$$

$$\Phi_B = -\tfrac{1}{2}\Phi_Q\tilde{Q}. \tag{28}$$

The noise vector and the noise transformation matrices

$$w[k] = [\xi_\Omega[k] \quad \xi_B[k]]^T, \tag{29}$$

$$\Psi = \begin{bmatrix} -\tfrac{1}{2}\tilde{Q} & 0_{(4\times3)} \\ 0_{(3\times3)} & I_{(3\times3)} \end{bmatrix}. \tag{30}$$

The process noise covariance matrix is thus

$$W[k] = \begin{bmatrix} \tfrac{1}{4}\tilde{Q}[k]\Xi_\Omega[k]\tilde{Q}^T[k] & 0 \\ 0 & \Xi_B[k] \end{bmatrix}, \tag{31}$$

where $\Xi_1[k]_{(3\times3)}$ is the noise covariance matrix of the angular velocity ${}^B\Omega$ to be derived in the next section.

3) State Noise Covariance Matrix. We have known from the Allan variance analysis that the dominant noise component of the ADXL-203 accelerometers is velocity random walk or a zero-mean Gaussian white noise process ξ_A. Without loss of generality, we assume all accelerometer axes have identical noise variance and are uncorrelated. The noise covariance matrix of the differential acceleration vector A_D from (4) is thus

$$\Xi_{AD} = E\left\{(\xi_{AD})(\xi_{AD})^T\right\} = 4\sigma_A^2 I_{(3\times3)}, \tag{32}$$

where σ_A^2 is the variance of ξ_A.

From Section II-B, the body angular velocity ${}^B\Omega$ is related to the differential acceleration vector A_D and its own time derivative ${}^B\dot{\Omega}$ by a nonlinear function,

$${}^B\Omega(t) = F\left(A_D(t), {}^B\dot{\Omega}(t)\right). \tag{33}$$

The noise of ${}^B\Omega(t)$ thus has a transformed white noise component $\xi_\Omega(t)$ associated with $A_D(t)$ and a transformed integrated white noise component $\xi_B(t)$ due to ${}^B\dot{\Omega}$.

In the absence of an analytical solution for (33), the scaled unscented transformation [22] is applied to compute the noise covariance of ${}^B\Omega$. The scaled unscented transformation is motivated by the notion of it is easier to approximate a probability distribution than it is to approximate a nonlinear function.

To find the noise covariance of $\xi_\Omega(t)$, we first disregard the effect of ${}^B\dot{\Omega}$. For the three-dimensional (n = 3) angular velocity vector, a set of at least seven ($2n$ + 1) weighted samples, called the sigma points, are generated. This sample set is zero mean and has covariance equal to the noise covariance of the differential acceleration vector A_D. The nonlinear transformation F is applied to each of the sigma points, and the covariance of the body angular velocity vector is approximated by the calculated covariance of the transformed sample set.

The sigma points S are selected by the algorithm:

$$S_0 = , \; c_0 = \kappa/(n+\kappa);$$
$$S_i = \left(\sqrt{(n+\kappa)\Xi_{AD}}\right)_i, \; c_i = 1/2(n+\kappa);$$
$$S_{i+n} = -\left(\sqrt{(n+\kappa)\Xi_{AD}}\right)_i, \; c_{i+n} = 1/2(n+\kappa); \quad (34)$$

where $\kappa \in \Re$ and $(n + \kappa) \neq 0$, $\left(\sqrt{(n+\kappa)\Xi_{AD}}\right)_i$ is the i^{th} row or column of the matrix square root of $(n + \kappa)\Xi_{AD}$, and c_i is the weight associated with the i^{th} sigma point.

The mean and noise covariance of ${}^B\Omega$ is computed as

$${}^B\overline{\Omega} = \sum_{i=0}^{2n} c_i \hat{S}_i , \quad (35)$$

$$\Xi_\Omega = \sum_{i=0}^{2n} c_i \left(\hat{S}_i - {}^B\overline{\Omega}\right)\left(\hat{S}_i - {}^B\overline{\Omega}\right)^T , \quad (36)$$

where $\hat{S}_i = F(S_i)$. (37)

The noise covariance of the angular velocity bias vector Ξ_B due to the noise in ${}^B\dot{\Omega}$ is found by repeating (34)–(37), with the effect of A_D disregarded.

D. The Measurement Model

1) Measurement Vector. The measurement vector is chosen to be the quaternion derived from the direction cosine matrix in (13),

$$z = \begin{bmatrix} q_{m0} \\ q_{m1} \\ q_{m2} \\ q_{m3} \end{bmatrix} = \begin{bmatrix} \sqrt{1 + c_{11} + c_{22} + c_{33}}/2 \\ (c_{23} - c_{32})/4q_{m0} \\ (c_{31} - c_{13})/4q_{m0} \\ (c_{12} - c_{21})/4q_{m0} \end{bmatrix}, \quad (38)$$

where c_{ij}, i, j = 1, 2, 3, are the elements of ${}^WC_B$.

2) Measurement Equation. The measurement equation is

$$z[k] = Hx[k] + v[k], \quad (39)$$

$$H = \begin{bmatrix} I_{(4\times4)} & 0_{(4\times3)} \\ 0_{(3\times4)} & 0_{(3\times3)} \end{bmatrix}, \quad (40)$$

where H is the measurement matrix and $v[k]$ is the measurement noise vector.

3) Measurement Noise Covariance Matrix. From Section II-D-3, the gravity noise vector has two components, a white noise process with variance associated with the accelerometers and a colored noise process due to the body acceleration of the instrument. The noise covariance of the unit gravity vector is given by

$$\Xi_G = \sigma_G^2 I = \frac{\sigma_W^2 + \sigma_C^2}{\|{}^B G\|^2} I , \quad (41)$$

where σ_G^2 is the variance of a component of gravity vector ${}^BG$ along a direction normal to the expectation value of the gravity vector, $E\{{}^BG\}$. σ_W^2 is the variance of the white noise process. Since there are two accelerometers in each sensing direction, we may compound the two sensor readings and reduce the noise variance by half,

$$\frac{1}{\sigma_W^2} = \frac{1}{\sigma_A^2} + \frac{1}{\sigma_A^2} \Rightarrow \sigma_W^2 = \tfrac{1}{2}\sigma_A^2 , \quad (42)$$

where σ_A^2 is the variance of ξ_A. σ_C^2 is the variance of the color noise process, the standard deviation σ_C is assumed to be equal to 1% of the magnitude of the gravity,

$$\sigma_C = 0.01\|G\| . \quad (43)$$

Although not strictly true, the components of colored noise vector are assumed to be uncorrelated.

We have found from the Allan variance analysis that the dominant noise component of the magnetometers is a vector of zero-mean Gaussian white noise processes ξ_M, where ξ_M and ξ_A are assumed to be uncorrelated. Assuming also that the three magnetometer axes are uncorrelated, the noise covariance of the magnetometer is thus $\sigma_M^2 I$. Therefore, the noise covariance of the unit magnetic North vector is given by

$$\Xi_N = \sigma_N^2 I = \frac{\sigma_M^2}{\|{}^B M\|^2} I , \quad (44)$$

where $\|{}^BM\|$ is the magnitude of the magnetic field.

The covariance of the error angle vector associated with the direction cosine matrix determined by the TRIAD algorithm can be shown to be in the form [15]

$$\Xi_\theta = \sigma_G^2 I + \frac{1}{\left\|{}^B z_W \times {}^B N\right\|^2}\left\{\left(\sigma_N^2 - \sigma_G^2\right){}^B z_W \, {}^B z_W^T + \sigma_G^2\left({}^B z_W \bullet {}^B N\right)\left({}^B z_W \, {}^B N^T + {}^B N \, {}^B z_W^T\right)\right\}, \quad (45)$$

where ${}^Bz_W$ is the negated normalized gravity vector defined in (10). The measurement noise covariance is thus

$$V[k] = \tfrac{1}{4}\tilde{Q}\Xi_\theta\tilde{Q}^T . \quad (46)$$

E. Kalman Filtering

1) Prediction. From (25), the predicted discrete state equation is

$$x^-[k] = \Phi[k]x[k-1]. \quad (47)$$

The projected error covariance is computed as

$$P^-[k] = \Phi[k]P^-[k-1]\Phi^T[k] + W[k]. \quad (48)$$

2) Filtering. The Kalman gain is obtained by compounding the noise covariance matrices of the state equation and measurement equation,

$$K[k] = P^{-}[k]H^{T}(HP^{-}[k]H^{T} + V[k])^{-1}. \quad (49)$$

The updated state vector with a new measurement is then

$$x[k] = x^{-}[k] + K[k](z[k] - Hx^{-}[k]), \quad (50)$$

and the updated error covariance is

$$P[k] = (I - K[k]H)P^{-}[k]. \quad (51)$$

V. Discussions

Besides the fundamental problem of integration drift associated with the inertial sensing technology, one other major challenge in implementing real-time orientation tracking is the 'true' real-time signal processing requirement of our application. The use of frequency selective filters to reduce the sensor noise would have caused a phase shift in the processed signal. As a result, the delay between the instantaneous instrument motion and the perceived motion defeats the objective of real-time active erroneous motion compensation. The direct consequence of this is the difficulty in obtaining high quality sensing information from the noisy sensors. This inherent problem in our application motivates the implementation of the proposed Kalman filter to decipher high quality sensing information from noisy sensors.

It is widely recognized that the most difficult part of performing sensor fusion via Kalman filtering is the formulation and the modeling of the problem with respect to the available sensor information. Most of the perceivable sources of sensing error are analyzed and modeled. However, to balance between modeling accuracy and computational efficiency, we have chosen to simplify and linearize some of the error dynamics, especially in cases where an explicit modeling would only bring about minute performance improvement.

The implementation and experimental results of the Kalman filter is presented in [11].

VI. Conclusion

We have presented the theory and modeling of a quaternion-based augmented state Kalman filter to perform real-time orientation tracking of a handheld microsurgical instrument. The proposed Kalman filter takes advantage of the motion dynamic during a microsurgery to combine the two sources of sensing information provided by the magnetometer-aided all-accelerometer IMU to extract non-drifting orientation estimates with improved resolution. Noise characteristics of the sensors are determined by the Allan variance analysis and the noise covariance matrices are derived either analytically or using scaled unscented transformation.

References

[1] E. Foxlin, M. Harrington, and Y. Altshuler, "Miniature 6-DOF inertial system for tracking HMDs," *In SPIE vol. 3362, Helmet and Head-Mounted Displays III, AeroSense*, Orlando, FL, April 13-14, 1998.

[2] E. Foxlin, "Inertial Head-Tracker Fusion by a Complementary Separate-Bias Kalman Filter," *Proc. VRAIS'96, IEEE*, pp.185-194, 1996.

[3] X. Yun, M. Lizarraga, E. R. Bachmann, and R. B. McGhee, "An Improved Quaternion-Based Kalman Filter for Real-Time Tracking of Rigid Body Orientation," *Proc. IEEE/RSJ Int. Conf. Intelligent Robots & Systems*, Las Vegas, pp.1074-1079,Oct 2003.

[4] E. R. Bachmann, X. Yun, D. McKinnery, R. B. McGhee, and M. J. Zyda, "Design and Implementation of MARG Sensors for 3-DOF Orientation Measurement of Rigid Bodies," *Proc. IEEE Int. Conf. Robotics & Automation*, Taipei, pp. 1171-1178, Sep 2003.

[5] D. Gebre-Egziabher, G. H. Elkaim, J. D. Powell, and B. W. Parkinson, "A Gyro-Free Quaternion-Based Attitude Determination System Suitable for Implementatoin using Low Cost Sensors," *Proc. IEEE Position, Location, and Navigation Symp.*, pp. 185-192, March 2000.

[6] H. Hehbinder and X. Hu, "Drift-Free Attitude Estimation for Accelerated Rigid Bodies," *Proc. IEEE Int. Conf. Robotics & Automation*, Seoul, pp. 4244-4249, May 2001.

[7] H. J. Luinge, "Inertial Sensing of Human Movement," *Ph.D. Thesis*, University of Twente, Twente University Press, Enschede, the Netherlands, 2002.

[8] C. N. Riviere, W. T. Ang, and P. K. Khosla, "Toward Intelligent Microsurgical Instrument," *IEEE Trans. Robotics and Automation*, Vol. 19, No. 5, pp. 793-800, Oct. 2003.

[9] W. T. Ang, P. K. Khosla, and C. N. Riviere, "Design of All-Accelerometer Inertial Measurement Unit for Tremor Sensing in Hand-held Microsurgical Instrument", *Proc. Int. Conf. Robotics and Automation*, Taipei, pp.1781-1786, Sep 2003.

[10] W. T. Ang, S. Y. Khoo, P. K. Khosla, and C. N. Riviere, "Physical Model of a Dual-Axis MEMS Accelerometer for Low-*g* Motion Tracking Applications", *Proc. Int. Conf. Robotics & Automation*, New Orleans, pp.1345-1351, May 2004.

[11] S. P. N. Singh and C. N. Riviere, "Physiological tremor amplitude during vitreoretinal microsurgery," *Proc. IEEE 28th Annual Northeast Bioengineering Conf.*, pp. 171-172, April 2002.

[12] G. Wahba, "Problem 65-1, A Least Squares Estimate of Satellite Attitude," *SIAM Review*, Vol. 7, No. 3, pp. 409, July 1965.

[13] J. L. Marins, X. Yun, E. R. Bachmann, R. B. McGhee, and M. J. Zyda, "An Extended Kalman Filter for Quaternoin-Based Orientation Estimation Using MARG Sensors", *Proc. IEEE/RSJ Int. Conf. Intelligent Robots and Systems*, Maui, pp. 2003-2011, 2001.

[14] M. D. Shuster and S. D. Oh, "Three-Axis Attitude Determination from Vector Observations," *J. Guidance, Control, and Dynamics*, Vol. 4, No. 1, pp. 70-77, Jan-Feb 1981.

[15] J. L. Farrell, J. C. Stuelpnagel, R. H. Wessner, and J. R. Velman, "Solution to problem 65-1: A least squares estimate of satellite attitude," *SIAM Review*, Vol. 8, No. 3, pp. 384-386, July 1966.

[16] I. Y. Bar-Itzhack and Y. Oshman, "Attitude Determination from Vector Observations: Quaternion Estimation," *IEEE Trans. Aerospace & Electronic Syst*, Vol. 21. No.1, pp.128-135, Jan. 1985.

[17] F. L. Markley and D. Mortari, "Quaternion attitude estimation using vector observations," *J. Astronautical Sciences*, Vol. 48, No. 2&3, pp. 369-380, Apr-Sep 2000.

[18] IEEE Standard Specification Format Guide and Test Procedure for Linear Single-Axis, Nongyroscopic Accelerometers, Annex I, IEEE Std 1293-1998.

[19] B. Barshan and H. F. Durrant-Whyte, "Inertial Navigation Systems for Mobile Robots", *IEEE Trans. Robotics and Automation*, Vol.11, No.3, pp. 328-342, Feb 1994.

[20] Y. F. Jiang and Y. P. Lin, "Error Analysis of Quaternion Tranformations," *IEEE Trans. Aerospace and Electronic Systems*, Vol. 27. No.4, pp.634-639, Jul. 1991.

[21] E. J. Lefferts, F. L. Markley, and M.D. Shuster, "Kalman Filtering for Spacecraft Attitude Estimation," *J. Guidance, Control, and Dynamics*, Vol. 5, No. 5, pp. 417-429, Sep-Oct 1982.

[22] S. Julier, J. Uhlmann, and H. F. Durrant-Whyte, "A New Method for the Nonlinear Transformation of Means and Covariances in Filters and Estimators," *IEEE Trans. Automatic Control*, Vol. 45, No.3, pp. 477-482, Mar 2000.